Proc Joint Conf 1976 Amer. Sect. ISES
+ Solar Energy Soc of Canada
Winnipeg 15-20/8/76

TECHNICAL FEASIBILITY OF A MODULAR DISH SOLAR ELECTRIC SYSTEM

B. P. Gupta
Energy Resources Center
Honeywell, Inc.
2600 Ridgway Parkway
Minneapolis, Minnesota 55413

ABSTRACT

The development of solar concentrators in recent years has produced a wide variety of collectors for the utilization of solar energy. This paper presents the technical feasibility of generating electricity by using a gas turbine in conjunction with a paraboloid of revolution (dish) solar concentrator. A conceptual design of a dish concentrator is obtained by parametrically examining the significant optical parameters. The optical performance analysis was conducted using the Honeywell Monte Carlo ray-trace simulation program. A thermodynamic analysis was conducted to evaluate the performance of four candidate thermodynamic cycles utilizing two working fluids. The cycles were the regenerative and non-regenerative Brayton cycles of both open and closed type. Air and helium were the working fluids for the open and closed type respectively. Analysis for the heat transfer from the solar radiation to the gas flowing in metal tubes at the receiver was also conducted. A paraboloid of revolution dish with a cavity receiver using an open air regenerative Brayton cycle turbine emerged as a technically feasible concept in the power range from 30 to 100 KW_{th} per module.

INTRODUCTION

An examination of the potential applications of solar energy indicates that a significant contribution to the energy economy can be made by the modular generation of electricity. Small scale power generation can have conceivably far reaching applications in both metropolitan and rural areas.

The design of advanced solar power systems and the subsequent energy conversion depends on the availability of economically competitive solar concentrators and heat engines. This paper discusses the concept of solar concentration and the simulation technique used to predict the performance of a dish-type concentrating collector. A model was developed on the principle of the Monte-Carlo technique to solve the integral equations. Simulations were carried out to analyze the optical and thermal performance of the dish collector which tracks the sun in two axes during the day. The dish collector concentrates the solar radiation on a receiver located at the focal point of the mirror. The power within the cavity receiver heats a working fluid which is used to operate a thermal engine to provide shaft power output. Hence the dish collector module consists of four major components, namely, the concentrator with tracking mechanism, the heat receiver, the thermal transport loop, and the turbine-generator. An artist's concept of the dish collector module is shown in Figure 1. Parametric analysis was conducted to determine the effect of the dish diameter, the focal length, and the concentration ratio on the net power at the receiver. The open regenerative Brayton cycle is schematically shown in Figure 2. Ideally, the air is initially compressed isentropically in a compressor. The compressed air is then heated at constant pressure partially in the regenerator and thereafter in the collector module heat receiver. Following the heat addition, the hot and compressed air is expanded isentropically through the turbine until it reaches a specified low end temperature. The turbine exhaust passes through the regenerator where it gives some of its heat to the counter-flowing compressed air before being exhausted to the atmosphere.

OPTICAL PERFORMANCE ANALYSIS

Computer Methodology

The system that is mathematically modeled by the code consists of

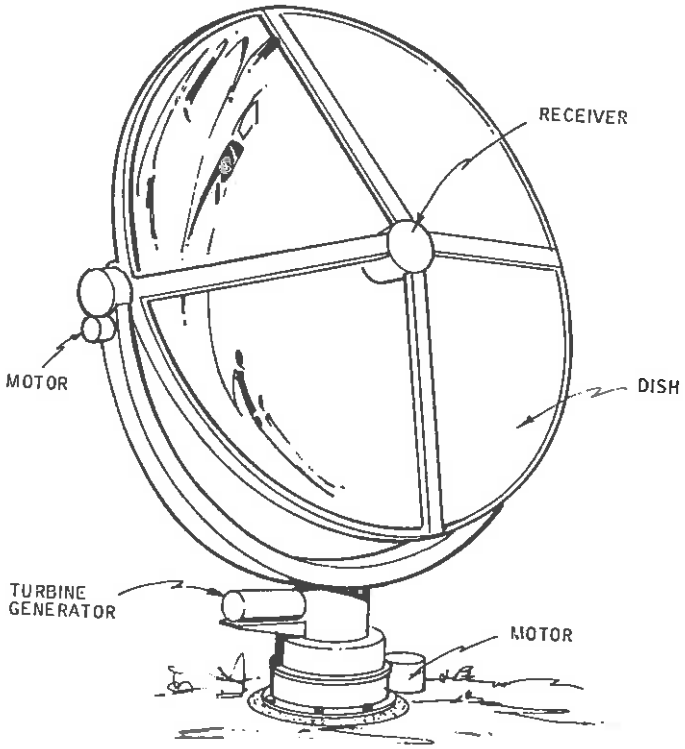

Figure 1. Artist's Concept of Dish Collector

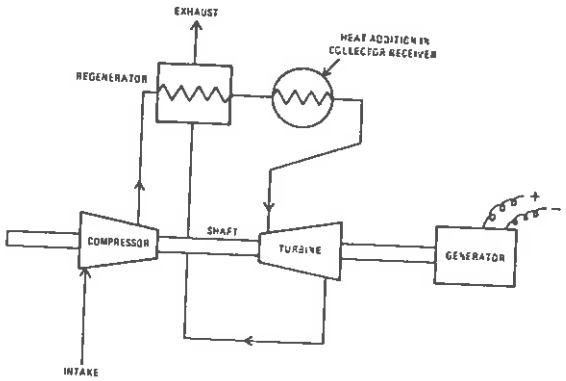

Figure 2. Open Cycle Regenerative Brayton Engine

a paraboloid of revolution mirror mounted on a two axis gimballed tracking system and a heat receiver. The generalized thermal optical performance characteristics of the system were formulated as an integration equation in conjunction with the Monte-Carlo technique. The vector algebra and the detailed description of the simulation code has been previously described in a NASA contract final report (1). Essentially, the amount of energy carried from any point on the sun's surface to any point on the heat receiver surface depends on the exact path of the ray through the optical interfaces on the collector. The mirror reflectance is a function of both the wavelength of the light in the ray and the incident angle of the ray on the mirror surface. The angle any ray makes with respect to each optical interface is a function only of the angular position on the solar disk from where the ray came (two-dimensional) and the impact point on the collector aperture plane (two-dimensional). Thus, for any wavelength and perfect optics, the energy carried from the sun to the receiver surface can be found by specifying the four coordinates of the ray, no matter how many optical elements there are within the optics train.

The ray-trace simulation code then evaluates a nine integral equation (1) for the paraboloid of revolution collector. In this integral equation two types of mirror uncertainties have also been included; one due to the collector tracking inaccuracy called the pointing error and the other due to the mirror quality called the slope error. The core of the analysis routine is a subroutine which evaluates the parameter E given in equation (2).

$$\bar{E}_p = \underbrace{\int_{\theta_1}\int_{\theta_2}}_{\text{tracking errors}} \underbrace{\int_{\phi_1}\int_{\phi_2}}_{\text{mirror imperfections}} P_{\theta_1} P_{\theta_2} P_{\phi_1} P_{\phi_2} \underbrace{\int_{\lambda}}_{\text{total spectrum}} \underbrace{\int_{X_1}\int_{X_2}}_{\text{collector aperture}} \underbrace{\int_{\delta_1}\int_{\delta_2}}_{\text{sun disk}} E \, d\delta_2 d\delta_1 \, dX_2 dX_1 \, d\lambda d\phi_2 d\phi_1 d\theta_2 d\theta_1 \tag{1}$$

$$E = E(X_1, X_2, \delta_1, \delta_2, \lambda, \theta_1, \theta_2, \phi_1, \phi_2) \tag{2}$$

here

δ_1, δ_2	are angular position coordinates on the sun disk
X_1, X_2	are impact point coordinates on the test plane
λ	is the wavelength
θ_1, θ_2	are pointing errors in two axes
ϕ_1, ϕ_2	are slope errors in two axes

To obtain the flux distribution within the cavity receiver another subroutine is added to the base program which counts the rays that go through the aperture opening of the receiver and hit the walls on the side of the cavity. The number of rays that hit a given wall segment are then counted, thereby defining the amount of energy concentrated in that segment.

Solar Collector Model

Figure 3 shows the dish collector modeled with a cavity receiver at its focus. The cavity receiver is a cylinder with a circular opening at the bottom through which the redirected flux enters the cavity formed behind the opening. This model includes the reradiation losses through the cavity opening and the loss due to shadowing from the receiver mounted at the focal point of the concentrator.

The heat losses due to convection for a cavity receiver is a second order effect with negligibally small magnitude and hence was not included in this analysis. This model was used to investigate the relationship between dish aperture diameter (D_c), concentration ratio (C_r), and rim angle (θ_r). The concentration ratio is defined here as the ratio of the collector aperture area to the area of the entrance aperture of the cavity receiver. The rim angle, as shown, is defined to be the angle between the optical axis and a line drawn from the focal point to the dish rim as shown in Figure 3. The variation of the rim angle thus takes into account a specific dish for each angle.

The dependence of θ_r on the dish depth (d) and the focal length (a) can be found from the equation of the parabola $X^2=4aY$. The coordinates of the rim $(D_c/2, d)$, when substituted into the equation, converts the equation in terms of the dish radius and depth

$$\frac{D_c^2}{4} = 4ad \qquad (3)$$

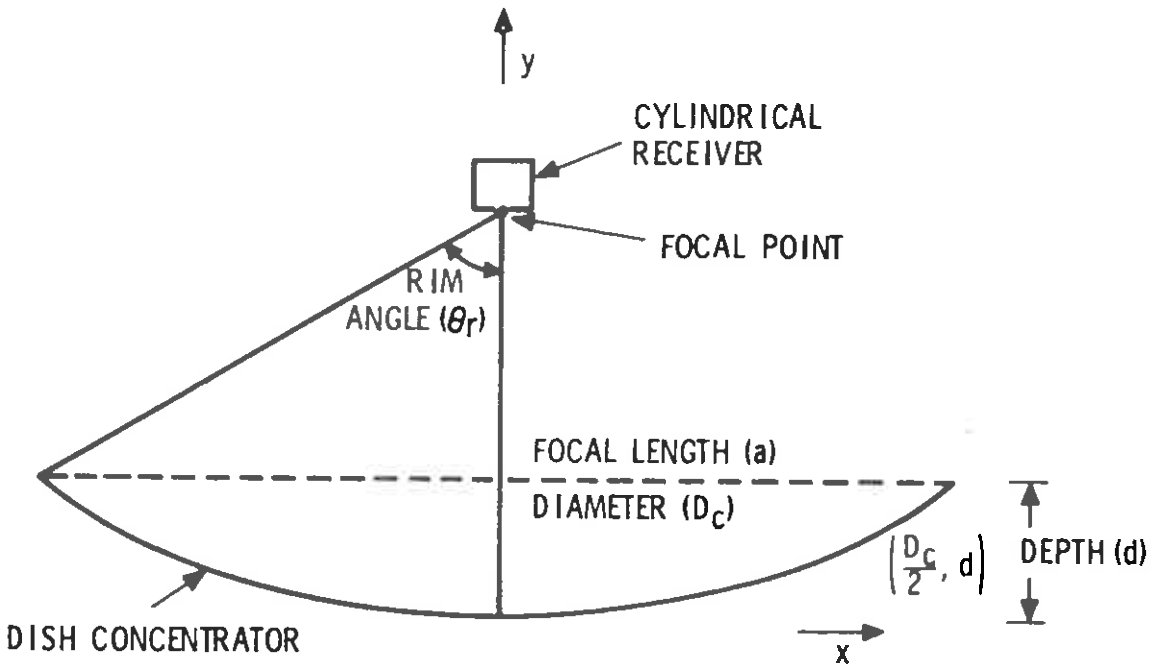

Figure 3. Dish Solar Collector Model

Then from the trigonometric right triangle function

$$\theta_r = \tan^{-1} \frac{Dc/2}{a-d} \tag{4}$$

Substituting Equation (3) into Equation (4) gives

$$\theta_r = \tan^{-1} \frac{2\sqrt{ad}}{a-d} \tag{5}$$

Equations (3) and (5) define the relationship between dish diameter, rim angle, focal length and dish depth. Table 1 shows the set of variable parameters which were used during the simulation. θ_r was varied from 30-90 degrees, C_r from 500-4000, and D_c from 5.5 to 16.5 meters.

In the parametric analysis of the collector system, two of the three variables were held constant while the third was varied systematically between the limits specified in Table 1. Pointing errors were fixed at

Table 1. Variable Parameter List

RIM ANGLES (θ_r)	COLLECTOR DIAMETERS (D_c), METERS	CONCENTRATION RATIOS (C_r)
30	5.5	500
40	7.3	1000
50	9.1	1500
60	11.0	2000
70	12.8	2500
80	16.5	3000
90		3500
		4000

0.1^{o} and slope errors at 0.15^{o}. These values were chosen as they are realistically achievable with conventional hardware. The cavity receiver geometry chosen for this analysis was a right circular cylinder 0.76 meter, both in diameter and height, with the receiver opening at the bottom coincident with the focal point of the concentrator. The cylindrical shape of the receiver was chosen for ease in developing the flux map software. The receiver diameter was chosen to accommodate an aperture opening of 0.66 meter for the worst case in which the collector diameter was 16.5 meters and the concentration ratio was 500. The height of the receiver was chosen to accommodate the length of tubing needed inside the receiver for the collection and transport of the thermal energy.

The heat losses due to re-radiation[2] and convection were calculated for the receiver by using the following equations respectively:

$$Q_r = \epsilon A_1 \sigma (T^4 - T_a^4) \tag{6}$$

where

Q_r = heat loss due to radiation

ϵ = emissivity of the radiating surface

A_1 = area of the radiating surface

σ = Stefan-Boltzmann constant

T = temperature of emitting surface

T_a = ambient temperature

and

$$Q_c = A_2 h (T - T_a) \tag{7}$$

where

Q_c = heat loss due to convection

h = heat transfer coefficient

T = temperature of the surface

T_a = ambient temperature

A_2 = area of the convective surface

An ambient temperature of 300°K and a wind velocity of 10 m/sec were used for the heat loss calculation from the above equations.

Simulation Results

For each of the points in the parameter list, the following variables were determined:

- power redirected by the collector aperture
- power entering the cavity receiver
- power retained within the receiver
- power distribution on the receiver cavity walls

The total power redirected is the amount of solar radiation intercepted by the collector aperture multiplied by the reflectance of the dish surface. The power entering the receiver cavity is slightly less than

the collected power because some rays get misdirected due to the dish surface irregularities.

The power retained within the receiver is that power which remains after the heat losses through the receiver aperture are considered and this retained power is also the net power in the cavity receiver. Finally, the power distribution is a flux map of the power on the receiver wall. The detailed results of the parametric study (3) are not being presented here for consideration of space. However, from all the data obtained it was determined that for the collector diameter range studied, the optimum concentration ratio and the optimum rim angle are 2000 and 60 degrees, respectively.

For the concentration ratio of 2000, the effect of rim angle variation on the net power for various collector diameters is shown in Figure 4.

The net power becomes sensitive to rim angle for larger collector diameters. Larger rim angle means that the receiver is located closer to the dish and would need larger aperture opening to receive the redirected energy. Larger aperture produces larger reradiation losses and the net power goes down. For smaller rim angles, the receiver is located farther away with more rays missing the aperture opening, therefore reducing the net power at the receiver.

Figure 5 shows the variation of net power as a function of concentration ratio for various collector diameters when the rim angle is held at 60^{o}. The curves dip sharply for smaller concentration ratios as the increased aperture area contributes to the increase in power loss.

For the optimum θ_r and C_r, the power entering the cavity receiver, the power lost, and the net power in the receiver as a function of aperture area are shown in Figure 6. The collector diameter is also shown for reference. This is a working curve which gives the collector diameter for a desired power level. In the range of collector diameters studied, the net power is seen to be directly proportional to the collector aperture area.

THERMODYNAMIC AND HEAT TRANSFER ANALYSIS

Analytic Approach

Analyses in three areas, namely: Brayton cycle turbine performance,

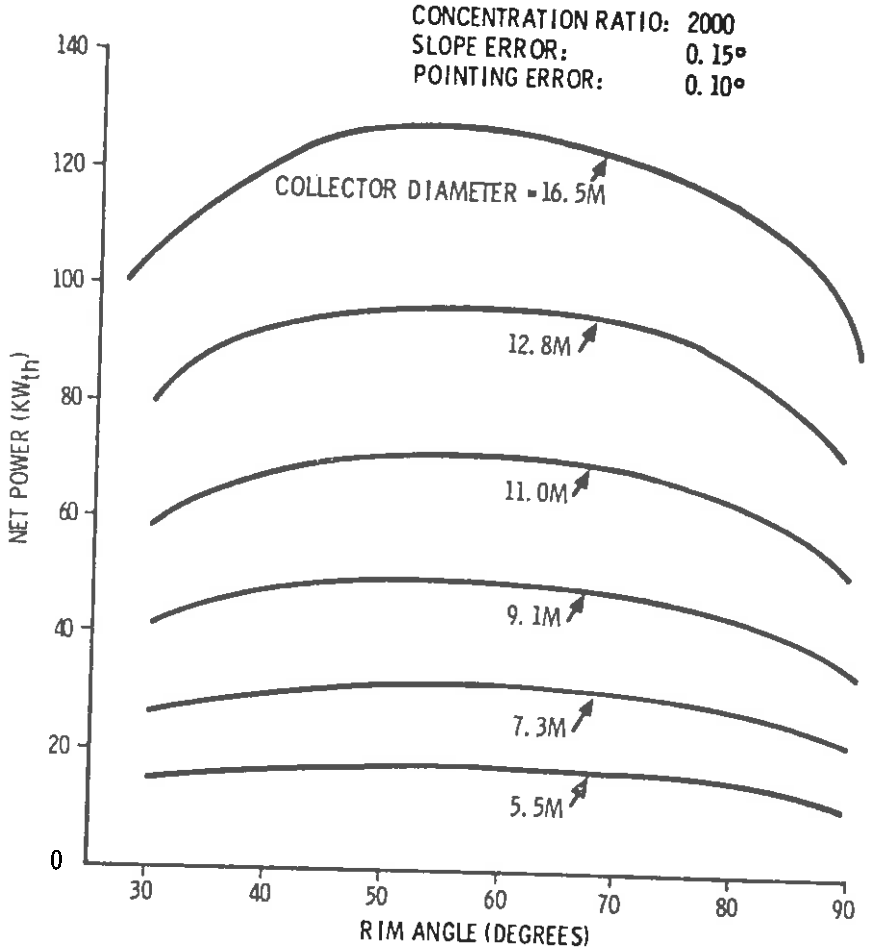

Figure 4. Net Power as a Function of Rim Angle

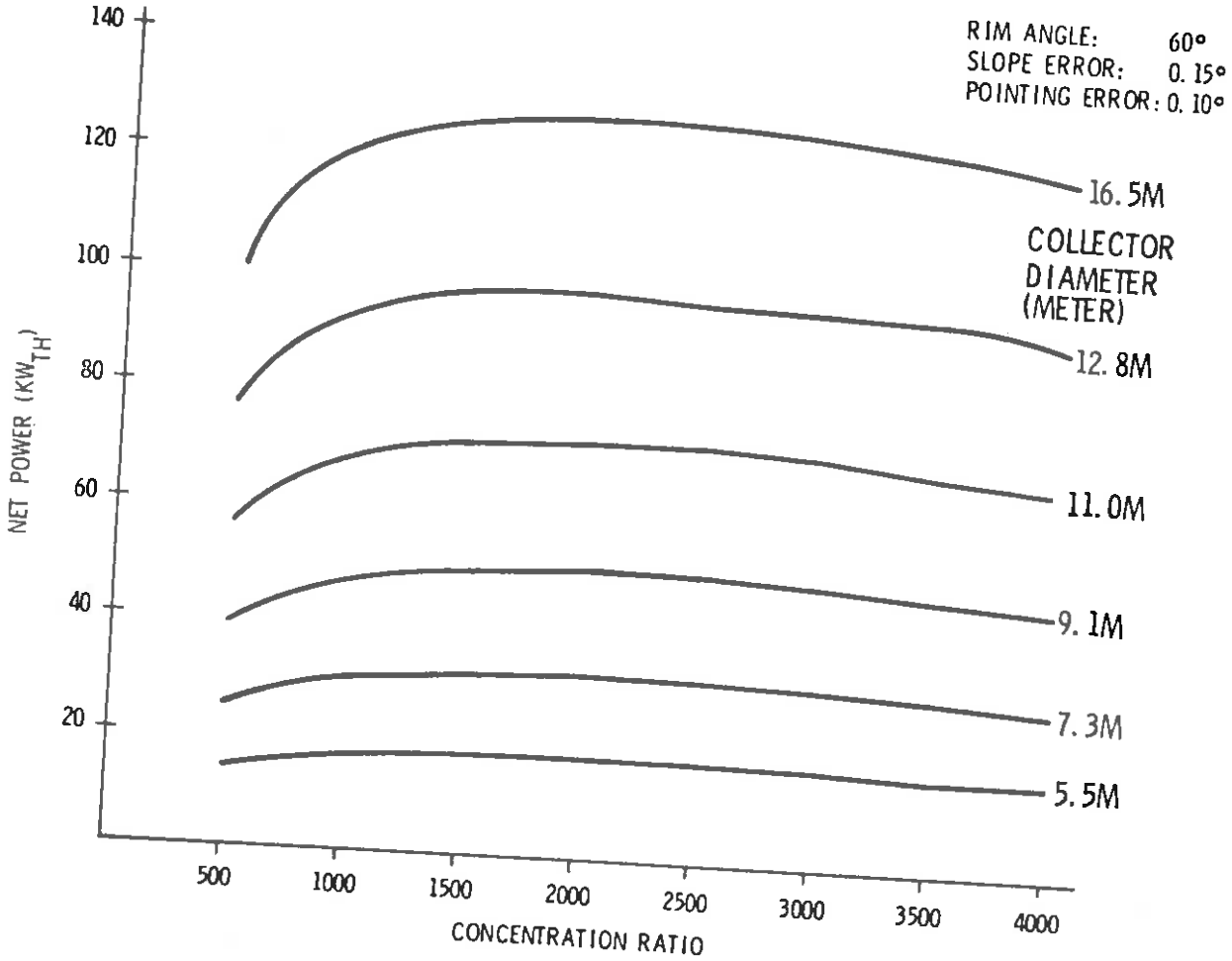

Figure 5. Net Power as a Function of Concentration Ratio

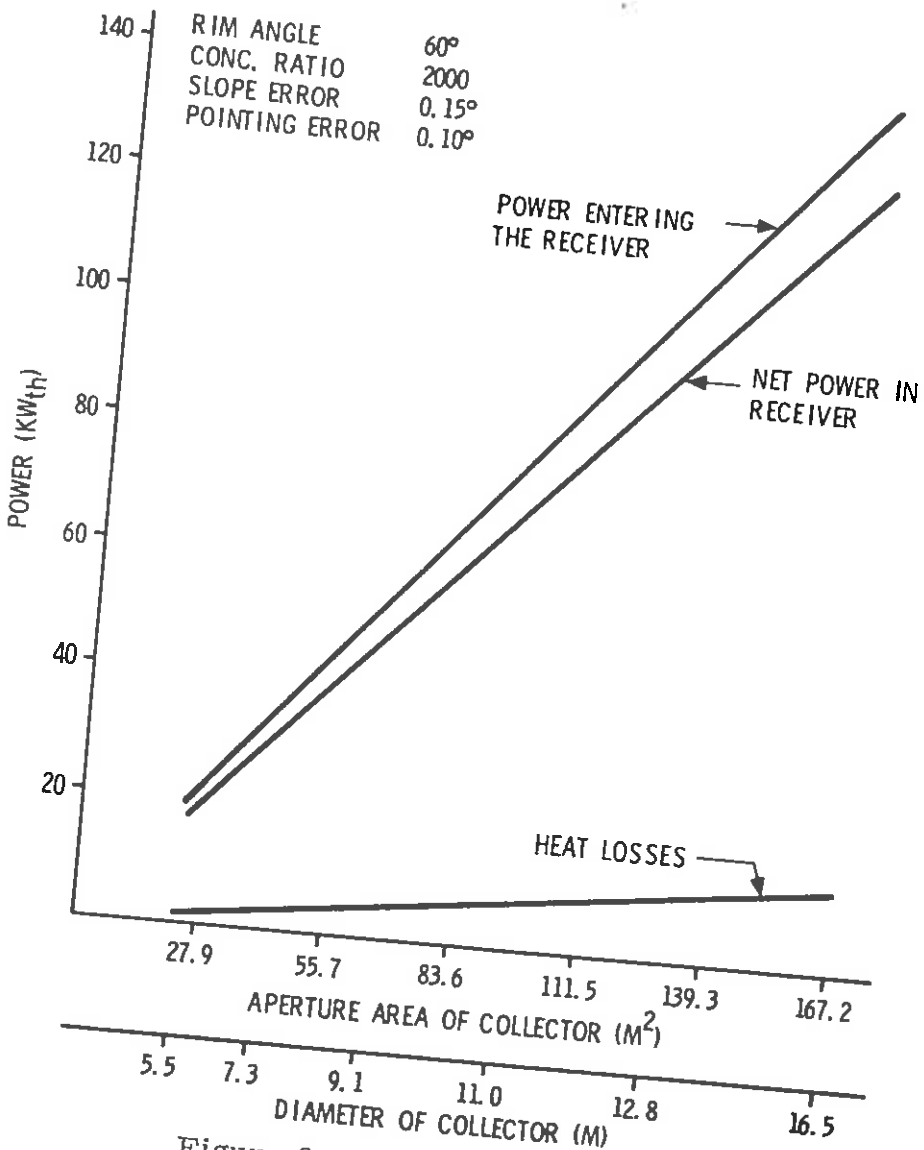

Figure 6. Power as a Function of Collector Area

heat transfer with direct heating, and heat transfer with indirect heating, were conducted to define the operating conditions for a high efficiency Brayton cycle application utilizing solar thermal energy.

The regenerative and non-regenerative Brayton cycles were analyzed for both air and helium as the working fluid. For reasonable initial fluid pressure and temperature, the cycles which provide the best performance within the range of expected cycle operating conditions were identified. This parametric analysis included losses and various component efficiencies so that realistic cycle efficiency could be predicted.

The heat transfer to the working fluid was parametrically analyzed for the case where the heat source tubes are directly heated by concentrated solar flux. The parameters varied were the tube dimensions, working fluid inlet velocities, and incident radiant flux intensity. The heat transfer results were integrated with the Brayton cycle analysis to determine the highest attainable cycle efficiency. Direct solar heating of the heat source tubes creates temperature variations around the tubes which define the operating temperature limits due to thermal stresses within the tubes.

Another area of investigation was the effect of indirect heating of the heat source tubes on the cycle efficiency. Provided this can be accomplished utilizing solar energy, it is seen as a technique for higher temperature operation with low thermal stresses in the heat source tubes.

Brayton Cycle Analysis

For an ideal Brayton Cycle, the efficiency increases with the pressure ratio. The cycle performance also increases when the maximum temperature before isentropic expansion is raised to the highest achievable point. However, this temperature is usually limited by the turbine materials or by the temperature attainable from the heat source. The regenerative Brayton Cycle has merit because the temperature of the turbine exhaust is greater than that of the compressor discharge. As a result of the regenerative heat exchange, the heat source must only raise the temperature of the working fluid part of the way, thus reducing the amount of heat input to the cycle.

The actual performance of a gas turbine differs from that of an ideal cycle primarily because of turbine and compressor irreversibilities

(inefficiencies) and pressure losses in gas flow passages, heat sources and heat exchangers. Therefore, the state points for a real gas turbine (dotted line) would be as shown in Figure 7.

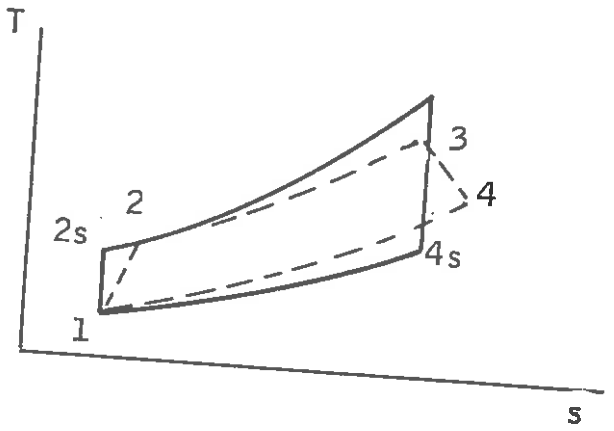

Figure 7. Comparison of Real and Isentropic Cycles

Using the nomenclature of Figure 7, the efficiencies of the turbine and compressor can be defined as follows:

$$\eta_c = \frac{h_{2s} - h_1}{h_2 - h_1} \qquad \text{where: } h \text{ is enthalpy of the working fluid at the state points indicated} \qquad (8)$$

$$\eta_c = \frac{h_3 - h_4}{h_3 - h_{4s}} \qquad (9)$$

One final characteristic of a real Brayton cycle should be recognized. The work required to drive the compressor is a substantial amount of the work produced by the turbine and, while it can vary greatly depending upon the cycle operating conditions, it is, in conventional turbines, on the order of two-thirds of the turbine output. This is particularly important in the consideration of real cycles because the effect of cycle losses is to increase the amount of compressor work required while reducing the amount of turbine work available.

Analytic Results -- The performance of the candidate prime mover systems was evaluated parametrically in an attempt to identify the cycle, and the operating conditions, best suited to efficient conversion of solar energy. The following parameters were evaluated:

- Turbine Inlet Temperature
- Compressor Pressure Ratio
- Heat Source Pressure Losses
- Initial Gas Pressure (ambient for the open cycle)
- Initial Gas Temperature (ambient for the open cycle)

Initial analyses were conducted to determine desirable and reasonable base conditions (initial gas pressure and temperature) for the cycle in question. After establishing the base conditions, the cycle performance was parametrically studied as a function of the three remaining parameters. The results of these analyses were interpreted and a set of cycle operating conditions were chosen that optimized cycle efficiency with the expected operating regime of the heat source. The component efficiencies used in the analysis were turbine efficiency of 0.85, compressor efficiency of 0.80, and regenerator effectiveness of 0.90. The results summarized here are for air as the working fluid. Detailed analytical results for both air and helium have been presented in a separate document (3).

Figure 8 shows the optimum pressure ratio determined for the air, regenerative cycle. The base conditions here are 14.6 psia and 70°F.

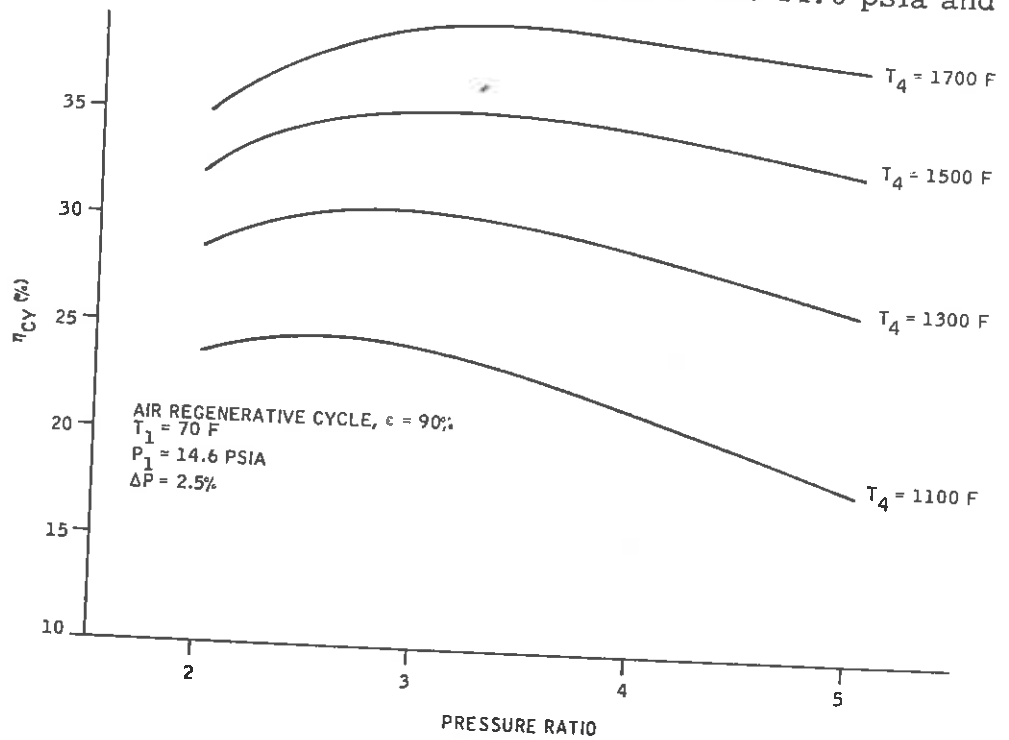

Figure 8. Cycle Efficiency as a Function of Pressure Ratio, Air Regenerative Cycle

A pressure ratio of 3.5 was determined to be optimum for this cycle. Figure 9 shows the increase in cycle efficiency with increasing turbine inlet temperature. For the case where the tubes are uniformly heated circumferentially, a temperature of 1950°F at the turbine inlet could be achieved with the resultant cycle efficiency of 43 percent. At 1700°F turbine inlet temperature, a cycle efficiency of 38 percent is obtained. Both efficiencies are for a 1.2 psia pressure drop.

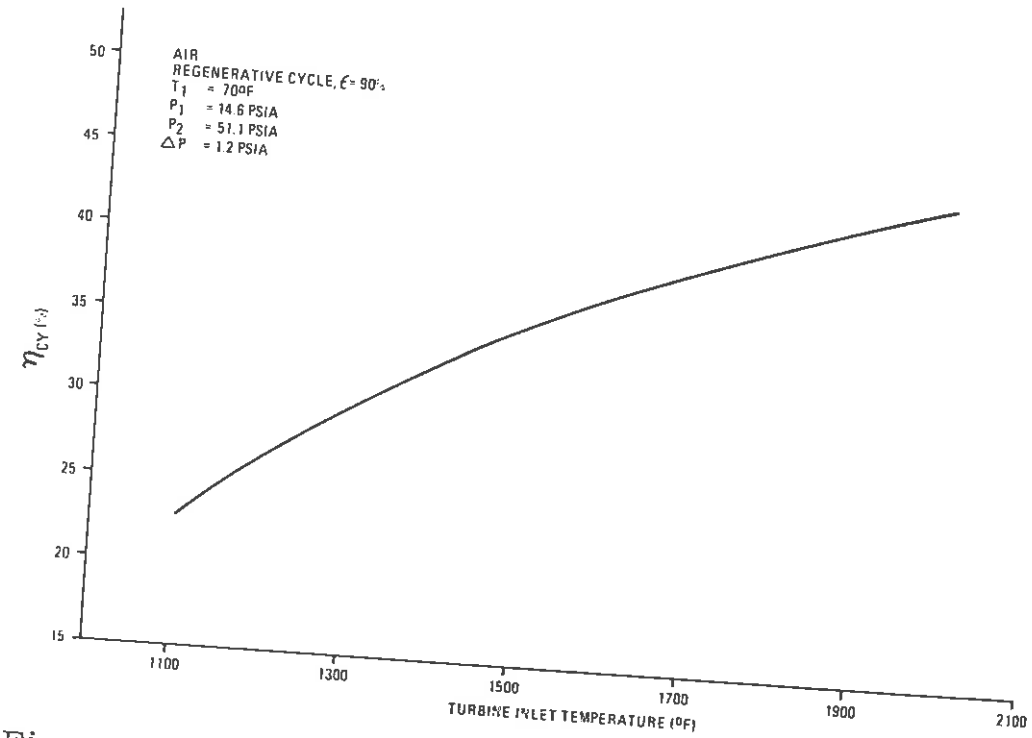

Figure 9. Cycle Efficiency as a Function of Turbine Inlet Temperature, Air Regenerative Cycle

The air, regenerative Brayton cycle achieves higher efficiency than the helium cycle examined for same turbine inlet temperatures. This is due to lower compressor inlet temperature (ambient air temperature) and because the lower operating pressure of the open cycle allows thinner-walled heat source tubing which decreases the thermal stresses allowing higher working fluid temperatures at the turbine inlet.

Heat Transfer Analysis

One method of heating the pressurized gas in the heat source is to

flow the gas through tubes and externally irradiate these tubes with redirected, concentrated solar energy. An analysis using computer simulation was performed to determine that combination of independent parameters which yield the highest cycle efficiency. The parameters studied were the tube inside diameter (I.D.), the diameter ratio (O.D. to I.D. ratio), the gas inlet velocity, and the solar flux intensity.

Two types of incident radiative fluxes were used, uniform and tailored. The uniform flux was held constant both circumferentially about the tube and axially along the tube. The tailored flux differs from the uniform flux in that it is not constant along the tube axis and changes in magnitude along the tube length to maintain the tube stresses everywhere just below the design limit. As with the uniform flux, the tailored flux is circumferentially uniform.

From the analysis, the same independent parameters were found to have identical optima for both types of incident radiative fluxes. The optimum tube I.D. is 0.25 inch, the optimum tube diameter ratio is 1.5, and the optimum inlet velocity is 50 feet per second. Tube I.D. of 0.25 inch was the smallest diameter considered in the study. It was seen that larger tube OD to ID ratios provide increased thermal efficiency but higher thermal stresses force the tube diameter ratio towards smaller values thus giving an optimal condition of 1.5 diameter ratio. The thermal heat transfer efficiency increases as the gas inlet velocity decreases. This is primarily due to the lower pressure drop at lower gas velocities.

The uniform flux assumption may seem academic but is viewed as one that is necessary for satisfactory cycle efficiency. Thermal stress considerations show that outlet temperatures of about 1700°F, a temperature non-uniformity around the tube of one percent will cause sufficient stress to fail the tube. When larger temperature non-uniformity is present, the gas outlet temperature would have to be lowered thus sacrificing operating cycle efficiency.

The non-uniformity of solar flux on the tubes in the heat source could be minimized by indirect heating through another medium. One such medium would be a fluid bath heated with solar flux. The thermal analysis was extended to briefly analyze such a concept.

Lithium Chloride (LiCl) was selected as the material for the bath concept primarily because of its availability and convenient melting point

(1130°F) and boiling point (2520°F). This selection was not intended to be optimum, but was made only to study a representative fluid.

The results show that when air is used in the cycle the optimum heat source parameters are: tube ID of 0.25 inch, tube OD of 0.29 inch, gas inlet velocity of 50 feet per second and the liquid bath temperature of 2000°F. Figure 10 shows that a cycle efficiency of 43.5 percent could be obtained under the above conditions.

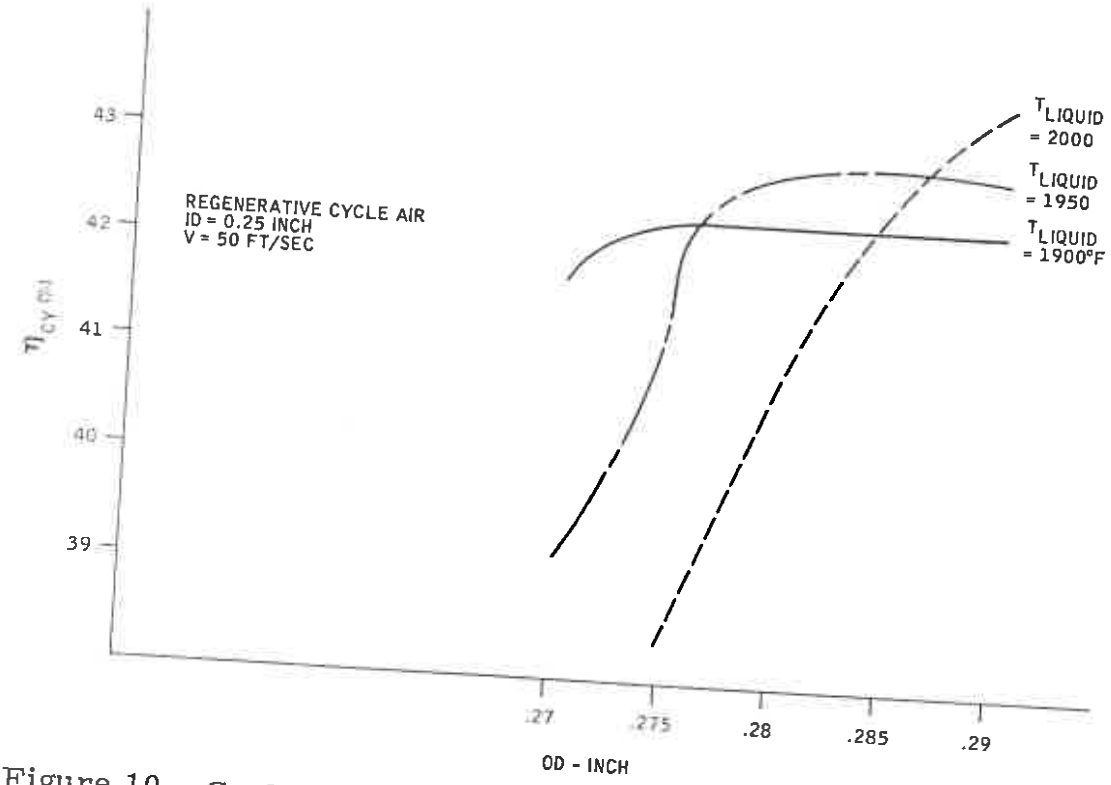

Figure 10. Cycle Efficiency as a Function of Tube Outside Diameter

It was determined that the required heat transfer from the liquid surrounding the tubing to the working fluid can be effected with reasonable tubing length. The tube length needed to attain the exit temperature with air is 3 feet with a pressure drop of less than 0.5 psia.

CONCLUSIONS

The simulation results show that the paraboloid of revolution dish collector could be used for concentrating solar energy into a cavity receiver to generate temperatures up to 1700°F, and thereby heat a

working fluid to operate a thermal engine. The complete size optimization of the dish collector can only be conducted by making a detailed design of the collector module and then conducting a cost and performance tradeoff of the collector system. For electrical power generation, the performance efficiency of a gas turbine operating on the Brayton cycle was also estimated during the program. A high overall efficiency could be obtained by using the concept of a dish solar concentrator and air Brayton cycle turbine to generate electrical power at the collector module and thus to satisfy small scale power needs at the point of use.

ACKNOWLEDGEMENTS

The analysis was conducted under NASA contract NAS3-19740. The author wishes to acknowledge the support and guidance received from Mr. Harvey Bloomfield, technical monitor for the National Aeronautics and Space Administration, Lewis Research Center, Cleveland, Ohio. The author also wishes to acknowledge the contribution made by the Honeywell engineering team and also by Black & Veatch, consulting engineers, Kansas City, Missouri.

REFERENCES

(1) Powell, J.C., et.al., "Dynamic Conversion of Solar Generated Heat to Electricity," NASA CR-134724, August 1974.

(2) Sparrow, E.M., and Cess, R.D., "Radiation Heat Transfer," Brooks/Cole Publishing Company, California, 1966.

(3) Gupta, B.P., et.al., "Technical Feasibility Study of Modular Dish Solar Electric Systems," NASA CR-135012, April 1976.